

RESEARCH PAPER



Atg1-dependent phosphorylation of Vps34 is required for dynamic regulation of the phagophore assembly site and autophagy in *Saccharomyces cerevisiae*

Yongook Lee^{a*}, Bongkeun Kim^{a*}, Hae-Soo Jang^a, and Won-Ki Huh^{ib a,b}

^aSchool of Biological Sciences, Seoul National University, Seoul, Republic of Korea; ^bInstitute of Microbiology, Seoul National University, Seoul, Republic of Korea

ABSTRACT

Macroautophagy/autophagy is a key catabolic pathway in which double-membrane autophagosomes sequester various substrates destined for degradation, enabling cells to maintain homeostasis and survive under stressful conditions. Several autophagy-related (Atg) proteins are recruited to the phagophore assembly site (PAS) and cooperatively function to generate autophagosomes. Vps34 is a class III phosphatidylinositol 3-kinase, and Atg14-containing Vps34 complex I plays essential roles in autophagosome formation. However, the regulatory mechanisms of yeast Vps34 complex I are still poorly understood. Here, we demonstrate that Atg1-dependent phosphorylation of Vps34 is required for robust autophagy activity in *Saccharomyces cerevisiae*. Following nitrogen starvation, Vps34 in complex I is selectively phosphorylated on multiple serine/threonine residues in its helical domain. This phosphorylation is important for full autophagy activation and cell survival. The absence of Atg1 or its kinase activity leads to complete loss of Vps34 phosphorylation in vivo, and Atg1 directly phosphorylates Vps34 in vitro, regardless of its complex association type. We also demonstrate that the localization of Vps34 complex I to the PAS provides a molecular basis for the complex I-specific phosphorylation of Vps34. This phosphorylation is required for the normal dynamics of Atg18 and Atg8 at the PAS. Together, our results reveal a novel regulatory mechanism of yeast Vps34 complex I and provide new insights into the Atg1-dependent dynamic regulation of the PAS.

Abbreviations: ATG: autophagy-related; BARA: the repeated, autophagy-specific Co-IP: co-immunoprecipitation; GFP: green fluorescent protein; IP-MS: immunoprecipitation followed by tandem mass spectrometry; NTD: the N-terminal domain; PAS: phagophore assembly site; PtdIns3P: phosphatidylinositol-3-phosphate; PtdIns3K: phosphatidylinositol 3-kinase; SUR: structurally uncharacterized region; Vps34[KD]: Vps34^{D731N}.

ARTICLE HISTORY

Received 28 July 2022
Revised 13 February 2023
Accepted 15 February 2023

KEYWORDS

Atg1; Atg8; Atg18; autophagy; nitrogen starvation; *Saccharomyces cerevisiae*; Vps34

Introduction

When cells are stressed or nutrients are depleted, one of the strategies that cells can employ is to “degrade” something to recycle essential materials and eliminate cytotoxic components. Macroautophagy/autophagy is a crucial catabolic process that can degrade a wide range of cellular components such as damaged organelles or proteins, thereby regenerating several building blocks for biomolecules and removing harmful components [1–3]. Autophagy starts with the formation of a cup-shaped membrane called the phagophore at the phagophore assembly site (PAS), where the integrated action of autophagy-related (Atg) proteins mediates expansion of the phagophore to create a double membrane autophagosome [4–6]. The autophagosome then finally engulfs desirable cargos and fuses with the vacuole or lysosome for degradation.

Among Atg proteins, Atg1 kinase is a key regulatory protein of autophagy that acts most upstream of autophagy signaling [7]. Atg1 kinase forms a stable protein complex with its regulatory subunit Atg13 [7–9]. Upon starvation, Atg13 is dephosphorylated in response to the inactivation of the target of rapamycin complex 1, and this allows the Atg1-Atg13 subcomplex to associate with the


Atg17-Atg31-Atg29 subcomplex to form heteropentameric Atg1 complex [10, 11]. In turn, this pentameric Atg1 complex forms a supramolecular, inter-complex assembly that serves as a PAS scaffold, and then Atg1 is fully activated [12]. Activated Atg1 kinase promotes the subsequent steps of autophagy by phosphorylating multiple Atg proteins, such as Atg4, Atg9, and Atg13, at the PAS [13–16]. Detailed studies on the Atg1 complex have made great strides in understanding the Atg1-dependent regulation of autophagy in recent decades. However, there are still many unanswered questions.

Vps34, the catalytic subunit of the phosphatidylinositol 3-kinase (PtdIns3K) complex, is another key regulator of autophagy that is conserved from yeasts to humans [17]. It synthesizes phosphatidylinositol-3-phosphate (PtdIns3P), an essential lipid for autophagy and endosomal trafficking [17,18]. In *Saccharomyces cerevisiae*, Vps34 forms two major complexes with distinct functions, namely, complex I and complex II [19]. Complex I is essential for autophagy activation while complex II is important for endosomal trafficking and vacuolar protein sorting [17–19]. Both complexes share the common subunits Vps15, Vps34, and Vps30. Complex I contains Atg14 as a specific subunit, which has been reported to determine

CONTACT Won-Ki Huh  wkh@snu.ac.kr  School of Biological Sciences, Seoul National University, Seoul, 08826, Republic of Korea

*These authors contributed equally to this work.

This article has been corrected with minor changes. These changes do not impact the academic content of the article.

 Supplemental data for this article can be accessed online at <https://doi.org/10.1080/15548627.2023.2182478>

© 2023 Informa UK Limited, trading as Taylor & Francis Group

the PAS localization of complex I, while Atg14 is replaced by Vps38 in complex II, which is crucial for its endosomal localization [20]. Atg38 is a fifth subunit of complex I which has been reported to hold the Vps15-Vps34 and the Atg14-Vps34 subcomplexes together, thereby stabilizing complex I [21]. The mammalian PtdIns3K complex I has been reported to undergo extensive phosphoregulation of its subunits by several kinases such as ULK1 [22–25], CDK1 [26], MTORC1 [27], and AMPK [28, 29]. Although ULK1, the mammalian homolog of Atg1, directly phosphorylates PIK3C3/VPS34 [22], the functional implications of this phosphorylation are not yet understood. Furthermore, our knowledge of the phosphoregulation of the yeast Vps34 complex is still very limited.

In this study, we report that Atg1-dependent phosphorylation of Vps34 is required for robust autophagy activity in *S. cerevisiae*. Following nitrogen starvation, Vps34 in Atg14-containing complex I is selectively phosphorylated on its helical domain, while Vps34 in Vps38-containing complex II is not. We found that this phosphorylation is important for full autophagy activation and cell survival under nitrogen starvation. The absence of Atg1 or its kinase activity leads to complete loss of Vps34 phosphorylation in vivo, and Atg1 is able to phosphorylate part of the helical domain of Vps34 in vitro, regardless of its associated complex type. We also provide evidence that the specific localization of Vps34 complex I to the PAS is one of the molecular bases for the complex I-specific phosphorylation of Vps34. In addition, Vps34 phosphorylation is required for the normal dynamics of Atg18 and Atg8 at the PAS. Collectively, our findings reveal a novel regulation mechanism of autophagy via phosphorylation of Vps34 complex

I and provide new insights into the Atg1-dependent dynamic regulation of the PAS.

Results

Vps34, the catalytic subunit of the PtdIns3K complex, is phosphorylated under nitrogen starvation

To investigate whether Vps34 undergoes posttranslational modification-based regulation in yeast, we analyzed the mobility of Vps34 by SDS-PAGE under autophagy-inducing conditions. Interestingly, the Vps34 band with reduced mobility appeared upon nitrogen starvation, and the amount of the upshifted Vps34 band increased as nitrogen starvation continued (Figure 1A). The upshift of the Vps34 band was positively correlated with gradually increasing autophagic activity along with nitrogen starvation as confirmed by the GFP-Atg8 processing assay (Figure 1B). In the GFP-Atg8 processing assay, autophagic activity can be measured by the emergence of free GFP moiety generated as a result of autophagy-dependent delivery of GFP-Atg8 to the vacuole, where the fusion molecules are degraded and relatively protease-resistant GFP accumulates [30]. By lambda protein phosphatase treatment, we identified the slower migrating band as a phosphorylated version of Vps34 (Figure 1C). By using kinase-defective Vps34^{D731N} mutant [31], we also confirmed that phosphorylation of Vps34 under nitrogen starvation does not require its own kinase activity, indicating that this

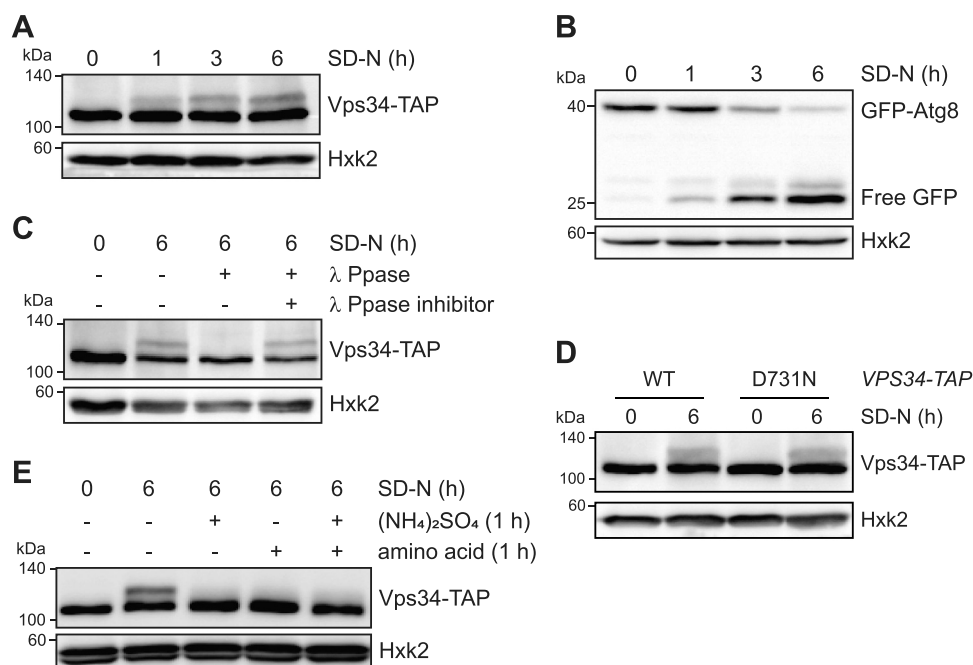


Figure 1. Vps34 is phosphorylated upon nitrogen starvation. (A) Cells expressing Vps34-TAP were grown to mid-log phase (SD-N 0 h) and incubated in SD-N medium for the indicated hours. Cell extracts were analyzed by immunoblotting with an anti-IgG antibody. (B) Cells expressing GFP-Atg8 were grown and starved as in (A). GFP-Atg8 processing was analyzed by immunoblotting with an anti-GFP antibody. (C) Vps34-TAP-expressing cells were grown to mid-log phase (SD-N 0 h) and incubated in SD-N medium for 6 h. Cell extracts were treated with lambda phosphatase with or without phosphatase inhibitors and analyzed by immunoblotting with an anti-IgG antibody. (D) Cells expressing the indicated Vps34 variants were grown to mid-log phase in SC medium (SD-N 0 h) and incubated in SD-N medium for 6 h. Immunoblotting was performed with an anti-IgG antibody. (E) Vps34-TAP-expressing cells were grown and nitrogen-starved as in (C). Then, ammonium sulfate (0.5% w:v) and/or amino acids were added for 1 h as described in the Materials and Methods. (A–E) Hxk2 was used as a loading control. The positions of molecular-mass markers (in kDa) are indicated to the left of the blots. A representative image of at least three independent experiments is shown.

phosphorylation is not autophosphorylation (Figure 1D). Notably, Vps34 was rapidly dephosphorylated when nitrogen sources were replenished (Figure 1E). These data suggest a link between Vps34 phosphorylation and autophagy activation.

Vps34 in complex I is specifically phosphorylated upon nitrogen starvation

Given that Vps34 is phosphorylated upon nitrogen starvation and Vps34 complex I is a central regulator of autophagy, we assumed

that Vps34 in complex I, not in complex II, is selectively phosphorylated under nitrogen starvation. To evaluate this hypothesis, we first deleted each component of Vps34 complexes and analyzed phosphorylation of Vps34 under nitrogen starvation. Interestingly, Vps34 phosphorylation was completely eliminated when the complex I-specific component *ATG14* or the common component *VPS15* or *VPS30* was deleted (Figure 2A). In contrast, deletion of *VPS38*, a specific subunit of Vps34 complex II, had no effect on phosphorylation of Vps34. Notably, the loss of Atg38, another subunit specific for Vps34 complex I, caused substantial, if not complete, inhibition of Vps34 phosphorylation (Figure 2A and

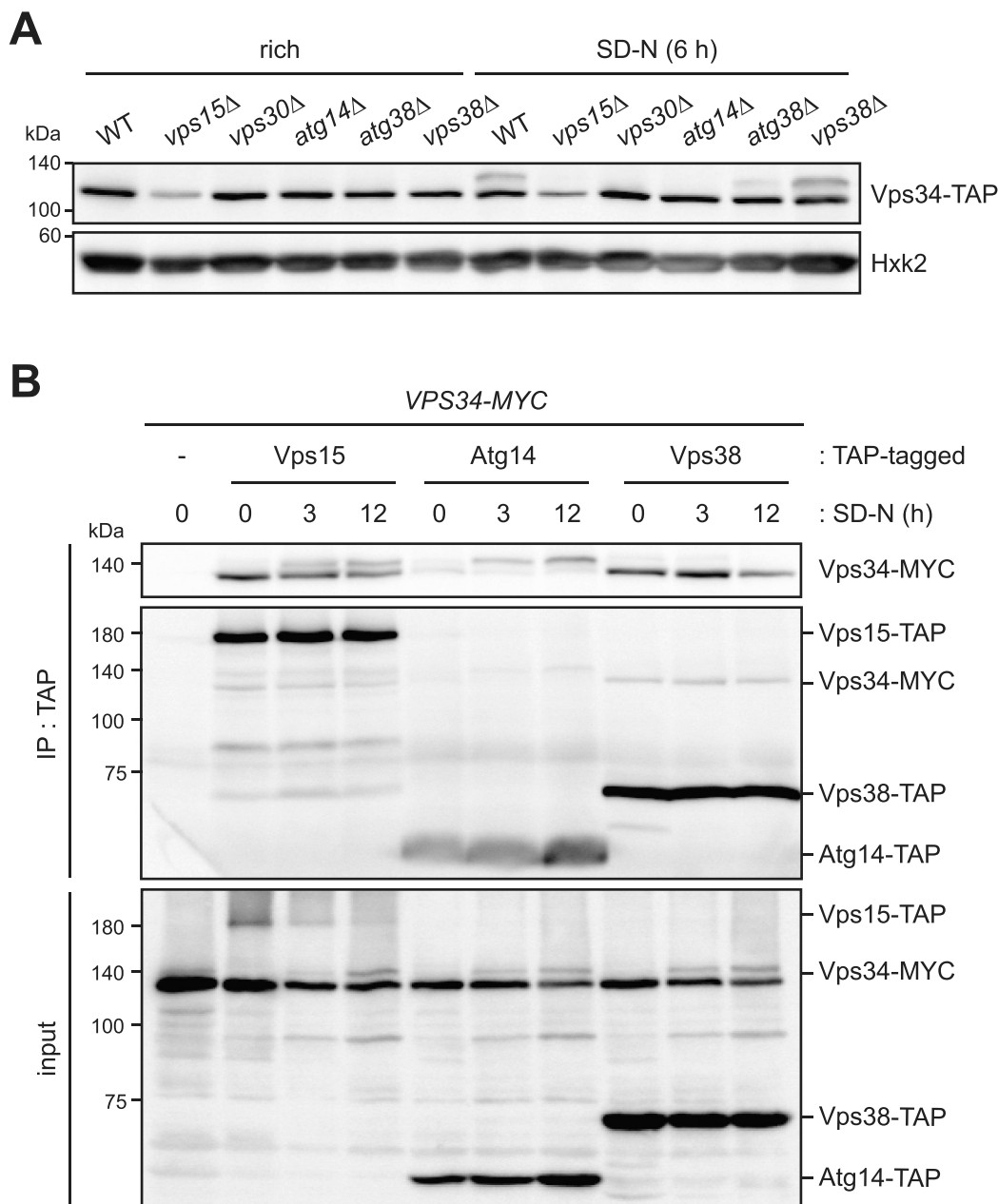


Figure 2. Vps34 complex I is specifically phosphorylated against complex II upon nitrogen starvation. **(A)** Vps34 phosphorylation was analyzed by immunoblotting with an anti-IgG antibody before (rich) and after nitrogen starvation (SD-N 6 h) in the indicated cells. Hxk2 was used as a loading control. **(B)** Cells expressing Vps34-MYC and the indicated TAP-tagged proteins were grown to mid-log phase (SD-N 0 h) and incubated in SD-N medium for the indicated hours. Cell extracts were immunoprecipitated using IgG-Sepharose beads and subsequently subjected to immunoblotting. The membrane was first developed with an anti-MYC antibody for Vps34-MYC detection (upper panel) and then with an anti-IgG antibody for the detection of TAP-tagged proteins (middle panel). *VPS34-MYC* cells expressing no TAP-tagged protein were used as a negative control. **(A and B)** The positions of molecular-mass markers (in kDa) are indicated to the left of the blots. A representative image of at least three independent experiments is shown.

S1.). To further confirm whether Vps34 in complex I is selectively phosphorylated under nitrogen starvation, we performed a coimmunoprecipitation (co-IP) assay. When Vps15, a common subunit of Vps34 complexes I and II, was pulled down, both phosphorylated and dephosphorylated forms of Vps34 were coprecipitated (Figure 2B). In agreement with our assumption, Vps34 coprecipitated with Atg14 was predominantly phosphorylated, whereas the majority of Vps34 coprecipitated with Vps38 was dephosphorylated. These data suggest that Vps34 in complex I is selectively phosphorylated in response to nitrogen starvation and that Vps34 phosphorylation is closely related to the autophagy regulation mechanism.

The helical domain of Vps34 is phosphorylated under nitrogen starvation

To investigate the function of Vps34 phosphorylation, we tried to identify the phosphorylated residues of Vps34 under nitrogen starvation by immunoprecipitation followed by tandem mass spectrometry (IP-MS). Although Vps34 has been reported to phosphorylate itself [31], phosphorylation of Vps34 under nitrogen starvation was not a result of autophosphorylation (Figure 1D). To prevent signals resulting from autophosphorylation, we used kinase-dead Vps34^{D731N} for mass spectrometric analysis. We identified one phosphorylated serine residue (S437, Figure S2A) and one phosphorylated peptide, the phosphorylation site of which could not be precisely determined (Figure S2B). Table 1 lists 12 phosphorylation site candidates of Vps34 that were identified in this study and in previous studies [13,32].

Based on the mass spectrometric analysis results, we constructed seven versions of nonphosphorylatable Vps34 mutants (Vps34[3A-1], Vps34^{S460A,S462A,S463A}; Vps34[3A-2], Vps34^{S465A,T467A,S468A}; Vps34[6A-1], Vps34^{S460A,S462A,S463A,S465A,T467A,S468A}; Vps34[3A-3], Vps34^{S428A,S437A,S445A}; Vps34[3A-4] Vps34^{S449A,T450A,S451A}; Vps34[6A-2], Vps34^{S428A,S437A,S445A,S449A,T450A,S451A}; Vps34[12A], in which all the above 12serine/threonine residues [hereafter “12S/T residues”] were mutated to alanine) and three versions of phosphomimetic Vps34 mutants (Vps34[6D-1], Vps34^{S460D,S462D,S463D,S465D,T467D,S468D}; Vps34[6D-2], Vps34^{S428D,S437D,S445D,S449D,T450D,S451D}; Vps34[12D], in which all the above 12S/T residues were mutated to aspartic acid) (Figure 3A). Notably, all these 12S/T residues are located in the helical domain of Vps34. We then analyzed the phosphorylation status of the Vps34 mutants by SDS-PAGE. As shown in Figure 3B, the Vps34 [3A-2], Vps34[3A-3] and Vps34[3A-4] mutants showed similar phosphorylation to that of wild-type Vps34 under nitrogen starvation, and phosphorylation of the Vps34[3A-1] mutant was slightly reduced compared to that of wild-type Vps34. Remarkably, under nitrogen starvation, phosphorylation of the Vps34[6A-1] and

Vps34[6A-2] mutants was severely compromised compared to that of wild-type Vps34, and the mobility shifts were almost entirely absent in the Vps34[12A] mutant. The mobility of the Vps34[6D-1] and Vps34[6D-2] mutants were slightly decreased even in nutrient-rich condition, and the Vps34[12D] mutant showed almost the same mobility with that of phosphorylated Vps34 (Figure 3B). These observations suggest that the 12S/T residues contain phosphorylation sites that are responsible for the mobility shift in SDS-PAGE upon nitrogen starvation.

The position of the 12S/T residues with respect to the overall Vps34 complex structure is indicated in Figure S3A, which is based on a crystal structure of Vps34 complex II (PDB ID: 5DFZ) [33] since there is no available high-resolution structure of Vps34 complex I. Interestingly, 10S/T residues out of the 12S/T residues (except for S428 and S437) belong to a structurally uncharacterized region (SUR) of the helical domain of Vps34 (from residues 438 to 478), and we found that this region is highly enriched in serine residues (Figure 3C). Furthermore, the regions in human PIK3C3/VPS34 and *Drosophila* Pi3K59F/Vps34 corresponding to the SUR in yeast Vps34 are also structurally undefined and highly enriched in serine residues (according to the PDB entries 5DFZ for yeast [33], 7BL1 for human [34], and 2X6H for *Drosophila* [35]), suggesting that the SUR is conserved in higher eukaryotes.

Phosphorylation of Vps34 promotes autophagy and yeast longevity under nitrogen starvation

To test whether phosphorylation of Vps34 is indeed required for proper autophagy activation, we examined the autophagic activity of cells expressing the nonphosphorylatable or phosphomimetic mutants of Vps34 by the Pho8Δ60 assay, which can quantitatively assess autophagic activity [36], and the GFP-Atg8 processing assay. As previously reported [19], deletion of *VPS34* resulted in a nearly complete loss of autophagic activity under nitrogen starvation (Figure 3D, E). When wild-type *VPS34* was reintroduced, autophagic flux was restored to a level comparable to that in wild-type cells, as expected. Cells expressing the Vps34[3A] mutants (Vps34[3A-1] to Vps34[3A-4]) also showed robust autophagy activity compared to cells expressing wild-type Vps34. However, cells expressing the Vps34[6A-1], Vps34[6A-2], or Vps34[12A] mutant were unable to fully restore autophagic flux. Reconstitution of the phosphomimetic Vps34 mutants (Vps34[6D-1], Vps34[6D-2], or Vps34[12D]) restored normal autophagic activity (Figure 3D, E, and S3B). All the above *vps34* mutants showed similar autophagic flux in nutrient-rich condition (Figure 3D and S3B, C). These results suggest that phosphorylation of the 12S/T residues in Vps34 is required for efficient autophagy activity under nitrogen starvation. To better understand the function of Vps34 phosphorylation, we also examined selective autophagy activity in Vps34[12A]- and Vps34[12D]-expressing cells by measuring free GFP molecules generated by vacuolar proteolysis of Pex11-GFP (pexophagy marker [37]) and Om45-GFP (mitophagy marker [38]). As previously described [37,39], deletion of *ATG36* and *ATG32*, which are essential genes for pexophagy and mitophagy, respectively, caused complete inhibition of corresponding selective autophagy as indicated by the inability to process Pex11-GFP or Om45-GFP into free GFP during prolonged nitrogen

Table 1. List of phosphorylation sites of Vps34.

Phosphorylation site	Reference
S437	This study
SISSESETSGTESLPVIVISPLAEFLIR*	This study
S428, S449, T450, S451	Lanz et al. [32]
S445, S449	Hu et al. [13]

*The specific phosphorylated residues were not identified. Residues mutated in Vps34[6A-1] are denoted in bold.

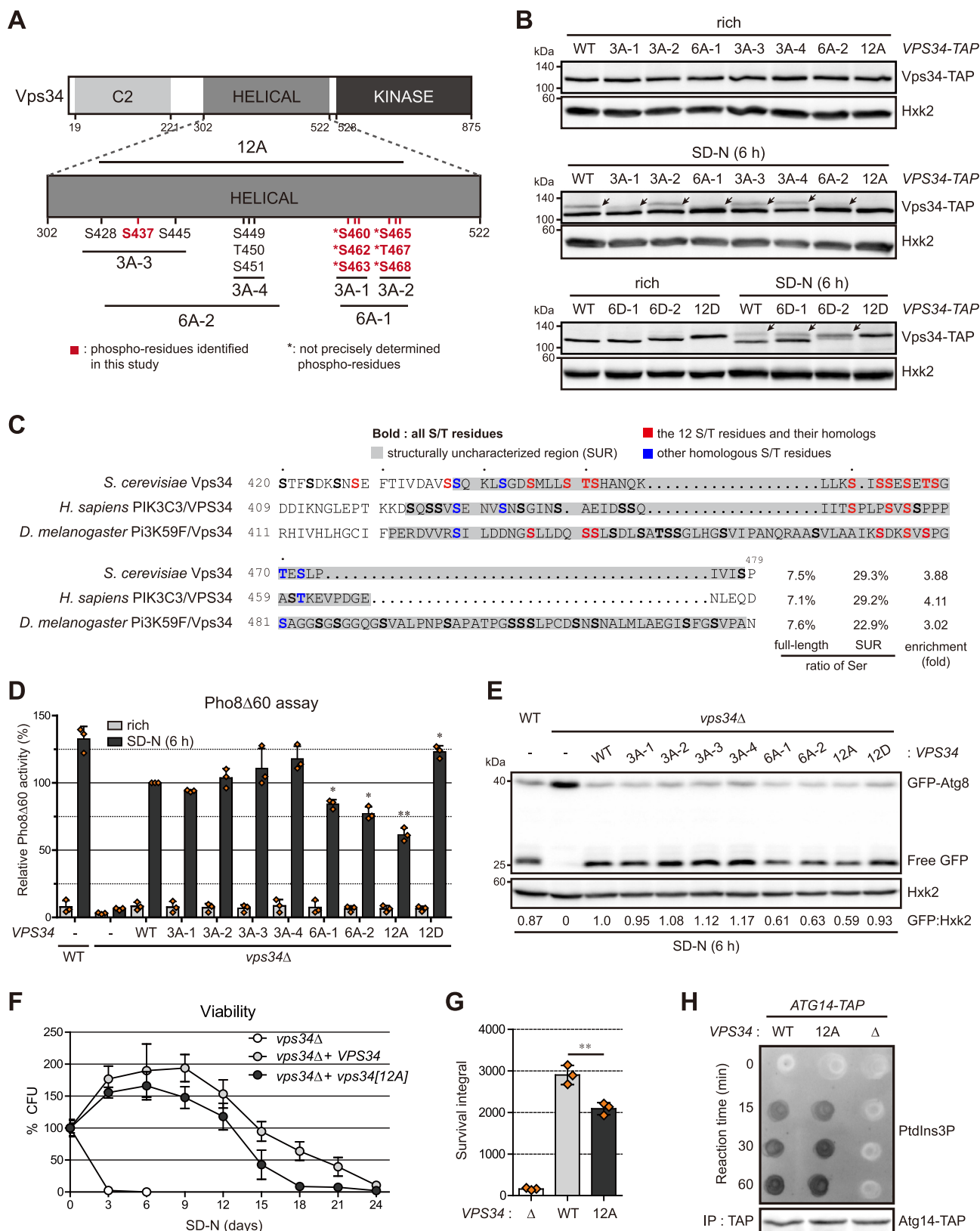


Figure 3. Vps34 phosphorylation on its helical domain promotes autophagy and cell survival under nitrogen starvation. **(A)** The nonphosphorylatable Vps34 constructs used in this study. The domain structure of Vps34 is represented as described in a previous study [33]. The designated S/T residues were substituted with alanine in the indicated Vps34 mutants. Red: phosphorylation residues identified in this study. Asterisks: phosphorylation residues which could not be precisely assigned. **(B)** Phosphorylation of the indicated Vps34 variants was analyzed by immunoblotting with an anti-IgG antibody before (rich) and after (SD-N 6 h) nitrogen starvation. Phosphorylated Vps34 is designated by arrows. **(C)** Sequence alignment of the SUR in Vps34 of *S. cerevisiae*, in PIK3C3/VPS34 of *H. sapiens*, and in Pi3K59F/Vps34 of *D. melanogaster* [33]. Bold: all S/T residues. Gray: the SUR. Red: the 12 S/T residues of yeast Vps34 and their homologous S/T residues. Blue: other homologous S/T residues. The ratios of serine in full-length Vps34 and the SUR are indicated to the right of each sequence. Enrichment values (the ratio of serine in the SUR divided by the ratio of serine in full-length Vps34) are also indicated. **(D)** Autophagy activity of the indicated cells was measured by Pho8Δ60 assay as described in the Materials and Methods. Values are normalized to that of *vps34Δ* cells expressing WT Vps34 in SD-N 6 h (set to 100). **(E)** Autophagy activity of the

starvation (Figure S3D, E). *vps34Δ* cells were also defective in both pexophagy and mitophagy. However, Vps34[12A]- and Vps34[12D]-expressing cells effectively processed Pex11-GFP and Om45-GFP to generate similar amounts of free GFP compared to wild-type cells, indicating that Vps34 phosphorylation is not required for mitophagy or pexophagy activity under nitrogen starvation.

Proper regulation of autophagy is necessary for extending cellular lifespan during prolonged nitrogen starvation [40]. To further characterize the physiological implications of Vps34 phosphorylation, we analyzed the chronological lifespan of cells expressing the Vps34[12A] mutant under prolonged nitrogen starvation, and the survival integral was then calculated as previously described [41,42]. As expected, cells expressing Vps34[12A] showed significantly decreased lifespans under chronic nitrogen starvation (Figure 3F, G). This result was further validated by flow cytometry using Phloxine B dye, which stains dead cells [43] (Figure S3F, G). Together, our findings suggest that Vps34 phosphorylation is specifically required for macroautophagic activity and promotes yeast longevity under nitrogen starvation.

Alanine substitutions of the 12S/T residues do not appear to affect the overall structure or stability of Vps34, as the amount of Vps34 mutants in cell extracts was comparable to that of wild-type Vps34 (Figure 3B). In addition, the Vps34[12A] mutant was able to properly perform Prc1/CPY (proteinase C) sorting (Figure S4A), which is a reliable indicator of a functional Vps34 complex II [19], and the binding abilities of Vps34[12A] with other complex subunits, namely, Atg14, Atg38, Vps38, Vps15, and Vps30, were similar to those of wild-type Vps34 (Figure S4B). To examine whether Vps34 phosphorylation is required for the catalytic activity of Vps34, we performed a lipid dot blot assay in which the PtdIns3K activity of Vps34 complex I can be measured in vitro by incubating an affinity-captured Atg14-immunocomplex with phosphatidylinositol in the presence of ATP [25]. Figure 3H demonstrates that the Vps34[12A] mutant showed PtdIns3K activity similar to that of wild-type Vps34, suggesting that Vps34 phosphorylation is dispensable for the enzymatic activity of Vps34 complex I. Together, these data suggest that alanine substitutions of the 12S/T residues do not impair the catalytic activity of Vps34 nor perturb the overall structure of Vps34 complexes.

Atg1 is an upstream kinase for Vps34 phosphorylation

Atg1 is a serine/threonine kinase that phosphorylates various autophagy proteins, such as Atg9 [15] and Atg19 [44], at the PAS upon autophagy activation. Furthermore, ULK1, the mammalian homolog of Atg1, has been shown to directly phosphorylate Ser249 of PIK3C3/VPS34, although the function of this

modification is not understood [22]. Thus, it is reasonable to presume that Atg1 kinase might directly phosphorylate Vps34 under nitrogen starvation. To verify this assumption, we first evaluated phosphorylation of Vps34 in cells with *ATG1*, *ATG13*, or *ATG17* deleted, which together comprise the Atg1 kinase complex and are necessary for Atg1 kinase activity. As expected, deletion of *ATG1*, *ATG13*, or *ATG17* completely disrupted Vps34 phosphorylation upon nitrogen starvation (Figure 4A). Conversely, Vps34 was normally phosphorylated in cells deleted for other downstream *ATG* genes (*atg3Δ*, *atg8Δ*, *atg11Δ*, *atg12Δ*, and *atg18Δ*) (Figure S5), indicating that a functional Atg1 complex, not a functional autophagy pathway, is required for Vps34 phosphorylation. Because Atg1 has a structural role in autophagy control as well as its own kinase activity [9,45], there still remains the possibility that other unknown kinases are recruited by Atg1 and phosphorylate Vps34. To check this possibility, we examined Vps34 phosphorylation in cells expressing Atg1^{D211A}, a kinase-dead variant of Atg1 [46]. As confirmed above, deletion of *ATG1* entirely eliminated phosphorylation of Vps34 upon nitrogen starvation, and reconstitution of wild-type Atg1 recovered Vps34 phosphorylation (Figure 4B). However, expression of Atg1^{D211A} could not restore this phosphorylation. This result demonstrates that the kinase activity of Atg1, not its structural role, is necessary for Vps34 phosphorylation under nitrogen starvation in vivo.

It has been recently shown that Atg1 can directly phosphorylate Vps34 in vitro, as confirmed by the incorporation of ³²P from [γ -³²P]-ATP [47]. To validate this, we performed an in vitro Atg1 kinase assay using immunoprecipitated Vps34-MYC and Atg13-TAP from *atg1Δ* cells as substrates and analyzed the mobility shifts of both proteins. As Vps34 is able to phosphorylate itself in vitro [31], we used kinase-dead Vps34^{D731N}-MYC (Vps34[KD]-MYC) as a substrate in order to exclude signals from autophosphorylation of Vps34 and specifically analyze Atg1-dependent phosphorylation. As previously reported [16,47], the affinity-purified Atg1 phosphorylated Atg13 but Atg1^{D211A} did not (Figure 4C, upper), as confirmed by the decreased mobility of Atg13 observed in both standard SDS-PAGE and Phos-tag SDS-PAGE, which increases the mobility shifts of phosphorylated proteins [48]. Although Vps34 was already phosphorylated to some extent before Atg1 reaction, clear band separation of Vps34 was induced by reaction with wild-type Atg1, while Atg1^{D211A} did not induce this mobility retardation (Figure 4C, lower). This data indicates that Vps34 can be a substrate of Atg1 kinase. Notably, in vitro Atg1 phosphorylation could not induce the mobility shift of Vps34 in standard SDS-PAGE.

We next investigated whether Atg1 can selectively phosphorylate Vps34 in complex I over Vps34 in complex II using Atg14-TAP- or Vps38-TAP-immunoprecipitates from Vps34[KD]-

indicated cells was measured by GFP-Atg8 processing assay. The relative ratio of free GFP to Hxk2 from three independent experiments was normalized against that of *vps34Δ* cells expressing WT Vps34 (set to 1.0) and is shown below each lane. (B and E) Hxk2 was used as a loading control. The positions of molecular-mass markers (in kDa) are indicated to the left of the blots. (F) Cells expressing the indicated Vps34 variants were grown to mid-log phase (Day 0) and incubated in SD-N medium for the indicated days. Survival values (CFU/ml) at each time point were normalized against the value on Day 0 of the corresponding strain. (G) The survival integral values in (F) are shown. (D, F, and G) The means of three independent experiments were plotted. The error bars indicate the standard deviations. Asterisks indicate significant differences compared with *vps34Δ* cells expressing WT Vps34 under the corresponding conditions (two-tailed Student's *t*-test): ***p* < 0.01, **p* < 0.05. (H) PtdIns3K activity of the indicated cells was analyzed. Atg14-TAP-immunoprecipitates were incubated with PtdIns and ATP for the indicated times. (B, E, and H) A representative image of at least three independent experiments is shown.

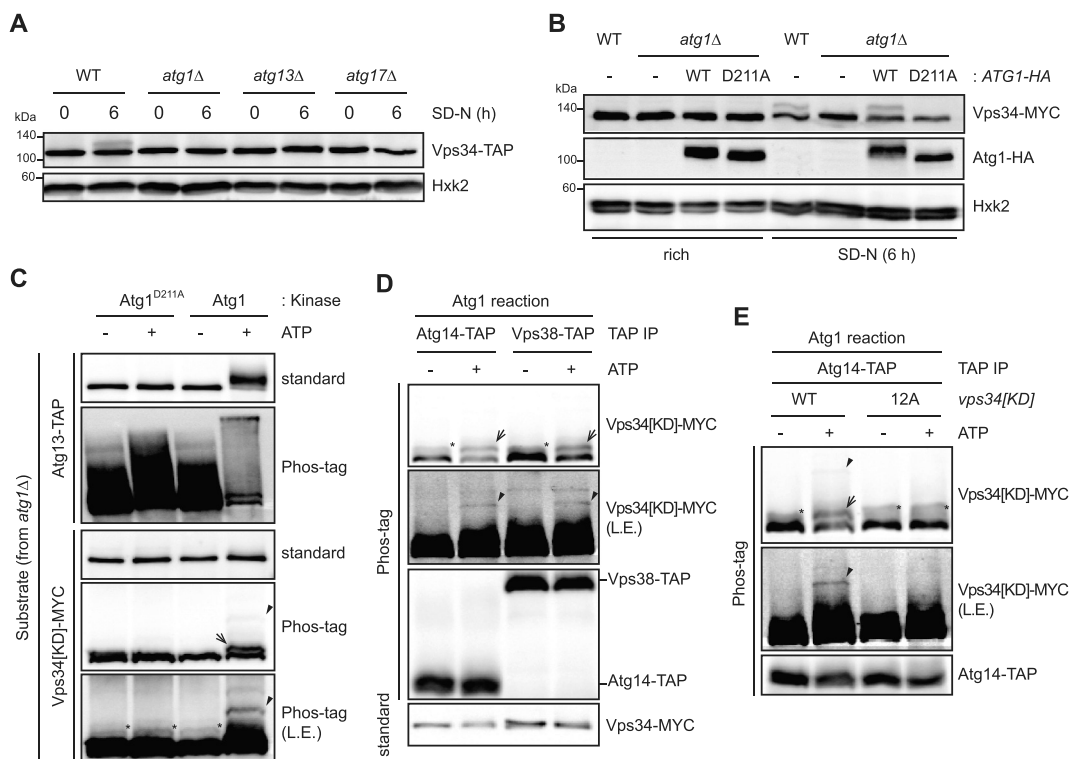


Figure 4. Atg1 is an upstream kinase for Vps34 phosphorylation. **(A)** WT, *atg1Δ*, *atg13Δ*, and *atg17Δ* cells expressing Vps34-TAP were grown to mid-log phase in YPD medium (SD-N 0 h) and incubated in SD-N medium for 6 h. Cell extracts were analyzed by immunoblotting with an anti-IgG antibody. **(B)** Cells expressing the indicated Atg1 variants were grown to mid-log phase in SC medium (rich) and incubated in SD-N medium for 6 h. Cell extracts were analyzed by immunoblotting with an anti-MYC antibody or anti-HA antibody. **(A and B)** Hxk2 was used as a loading control. The positions of molecular-mass markers (in kDa) are indicated to the left of the blots. **(C)** In vitro Atg1 reaction was performed using Vps34[KD]-MYC- and Atg13-TAP-immunoprecipitates as substrates. Atg13-TAP was used as a positive control. **(D)** In vitro Atg1 reaction was performed using Atg14-TAP- and Vps38-TAP-immunoprecipitates as substrates. **(E)** In vitro Atg1 reaction was performed using Atg14-TAP-bound Vps34[KD]-MYC (WT) and Vps34[12A+KD]-MYC (12A) as substrates. **(C-E)** An in vitro kinase assay was performed as described in the Materials and Methods. The results from Phos-tag SDS-PAGE and standard SDS-PAGE are indicated beside the blots. Asterisks indicate already phosphorylated protein bands before Atg1 reaction. Arrows and arrowheads indicate Atg1-dependent phosphorylation bands. L.E. indicates long exposure. **(A-E)** A representative image of at least three independent experiments is shown.

MYC-expressing *atg1Δ* cells as substrates. Figure 4D demonstrates that Atg1 reaction could induce the mobility shift of Vps34[KD] contained in Atg14-TAP-immunoprecipitates, indicating that Atg1 can phosphorylate Vps34 in complex I. Remarkably, Atg1 could also phosphorylate Vps34 in Vps38-TAP-immunoprecipitates in a similar manner to Vps34 in complex I. This result suggests that Atg1 is able to phosphorylate Vps34 in both complex I and II in vitro. Next, we examined whether Atg1 directly phosphorylates the 12S/T residues using Atg14-bound Vps34[KD]-MYC and Vps34[12A+KD]-MYC as substrates. In agreement with Figure 4D, Atg1 could phosphorylate Vps34[KD] in complex I (Figure 4E). Interestingly, however, the Atg1-induced mobility shift that was detectable with Vps34[KD] was not observed with Vps34[12A+KD], indicating that the 12S/T residues contain the Atg1 target residues. Collectively, these data suggest that in vivo phosphorylation of Vps34 is dependent on Atg1 kinase activity and that Atg1 can directly phosphorylate some of the 12S/T residues of Vps34 in vitro, even though Atg1 does not phosphorylate all of the residues responsible for the mobility shift of Vps34. In addition, Atg1 does not seem to discriminate the type of Vps34 complex as a substrate in vitro.

Localization of Vps34 to the PAS is necessary for the complex I-specific phosphorylation of Vps34 under nitrogen starvation

The above result that Atg1 can phosphorylate both Vps34 complexes in vitro prompted us to ask about a molecular mechanism that enables the complex I-specific phosphorylation of Vps34. Given that Atg1 phosphorylates multiple substrates at the PAS and that Vps34 complex I localizes at the PAS upon autophagy induction, it is likely that the PAS is where Atg1-dependent phosphorylation of Vps34 takes place; therefore, the PAS localization of Vps34 might be crucial for the complex I-specific Vps34 phosphorylation. To test this possibility, we examined Vps34 phosphorylation upon deletion of *ATG9*, which considerably impairs the localization of complex I to the PAS [49,50]. As expected, phosphorylation of Vps34 was remarkably decreased in *atg9Δ* cells (Figure 5A). To test whether the PAS localization of Vps34 complex I is indeed impaired in *atg9Δ* cells, we examined the targeting of Atg14, a specific subunit of Vps34 complex I, to the PAS by measuring Atg14 puncta colocalized with Atg13, a PAS

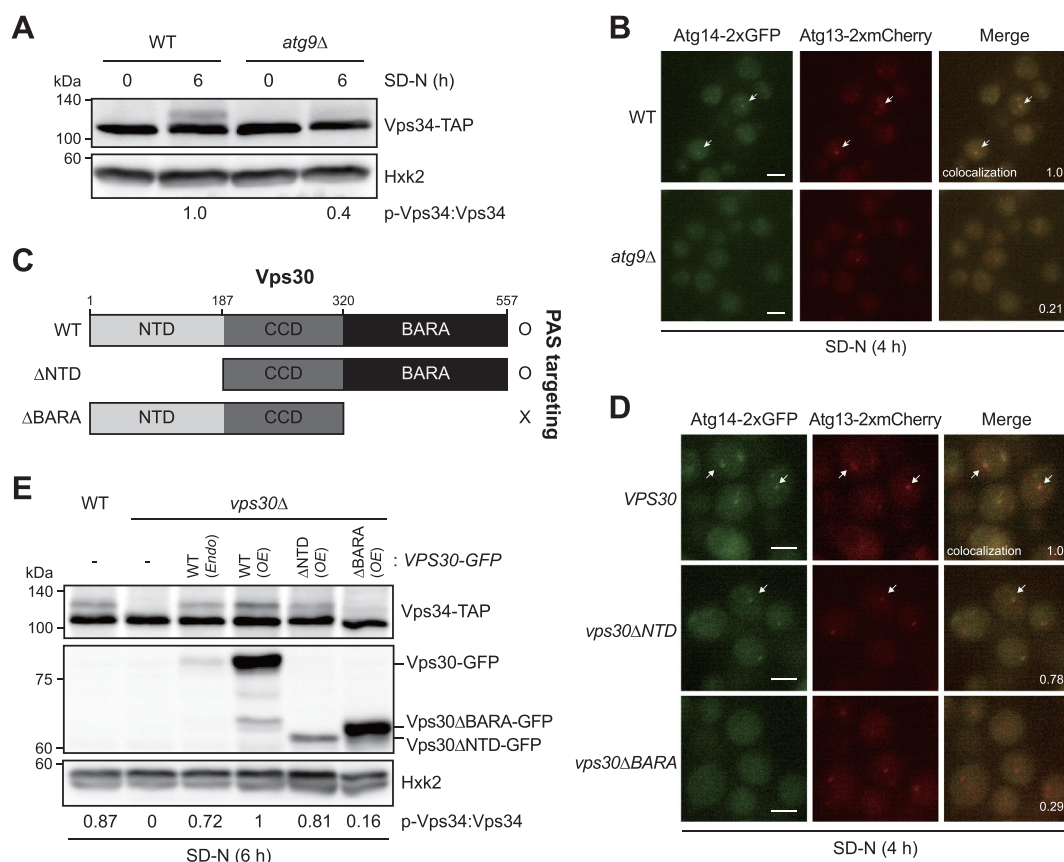


Figure 5. Targeting of Vps34 to the PAS is necessary for Vps34 phosphorylation. **(A)** WT and *atg9Δ* cells expressing Vps34-TAP were grown to mid-log phase in YPD medium (SD-N 0 h) and incubated in SD-N for 6 h. The relative ratio of phosphorylated Vps34 to unphosphorylated Vps34 was normalized against that of WT cells (set to 1.0) and is shown below each lane. **(B)** Colocalization of Atg14-2xGFP and Atg13-2xmCherry in WT and *atg9Δ* cells was examined after 4 h of incubation in SD-N medium. **(C)** Vps30 truncation mutants used in this study. Δ NTD, Vps30 without the NTD. Δ BARA, Vps30 without the BARA domain. **(D)** Colocalization of Atg14-2xGFP with Atg13-2xmCherry in the indicated cells was examined as in (B). **(B and D)** The PAS localization of Atg14 was analyzed by measuring the ratio of Atg13-2xmCherry puncta colocalized with Atg14-2xGFP. The relative colocalization value normalized against that of WT cells (set to 1.0) is shown on the lower right corner of each merged image. At least 300 Atg13-2xmCherry puncta were analyzed for each strain. Colocalized puncta are indicated by white arrows. Scale bars: 2 μ m. **(E)** Vps34 phosphorylation was examined in cells expressing the indicated Vps30 variants after 6 h of incubation in SD-N medium. Vps30 variants were expressed under either endogenous promoter (Endo) or *ADH1* promoter (OE). The relative ratio of phosphorylated Vps34 to unphosphorylated Vps34 was normalized against that of WT (OE) cells (set to 1.0) and is shown below each lane. **(A and E)** Cell extracts were analyzed by immunoblotting as described in the Materials and Methods. Hxk2 was used as a loading control. The positions of molecular-mass markers (in kDa) are indicated to the left of the blots. A representative image of at least three independent experiments is shown.

scaffold protein [12], under nitrogen starvation. Consistent with previous reports [49,50], Atg14 failed to properly localize at the PAS in *atg9Δ* cells under nitrogen starvation (Figure 5B). These data indicate that Atg9 is required for Vps34 phosphorylation under nitrogen starvation.

To rule out the possibility that unidentified functions of Atg9 might influence Vps34 phosphorylation, we used a different strategy to disrupt complex I localization to the PAS. Vps30 consists of three domains: the N-terminal domain (NTD), the coiled-coil domain (CCD), and the β - α repeated, autophagy-specific (BARA) domain [51]. It has been reported that the BARA domain of Vps30 is critical for the recruitment of complex I to the PAS, whereas the NTD of Vps30 is dispensable for the PAS targeting of complex I [51]. Thus, we made use of Vps30 truncation mutants to specifically block the PAS localization of complex I (Figure 5C). Consistent with a previous report [51], deletion of the BARA domain severely compromised the

PAS targeting of Atg14, whereas *vps30ΔNTD* cells showed robust, albeit slightly reduced, Atg14 localization to the PAS (Figure 5D). Subsequently, phosphorylation of Vps34 in cells expressing Vps30 truncation mutants was measured upon nitrogen starvation. We took advantage of the overexpression system under the *ADH1* promoter to express Vps30 truncation mutants because deletion of the NTD considerably destabilized Vps30 under nitrogen starvation (Figure 5E). As described in Figure 2A, deletion of *VPS30* caused complete inhibition of Vps34 phosphorylation under nitrogen starvation. When wild-type Vps30 was reintroduced, regardless of the expression level, phosphorylation of Vps34 upon nitrogen starvation was almost fully restored. Similarly, the Vps34 phosphorylation levels in *Vps30ΔNTD*-expressing cells were comparable to those of wild-type cells. Notably, however, restoration of *Vps30ΔBARA* in *vps30Δ* cells could not recover phosphorylation of Vps34 under nitrogen starvation, indicating that the BARA domain of Vps30

is required for Vps34 phosphorylation. Taken together, these data suggest that the PAS localization of Vps34 complex I is necessary for Vps34 phosphorylation under nitrogen starvation.

Atg1-mediated Vps34 phosphorylation is required for regulation of normal PAS dynamics under nitrogen starvation

It has been previously shown that Atg1 phosphorylates Atg9 and this phosphorylation promotes Atg18 recruitment to the PAS [15]. Papinski and Kraft [52] proposed that Atg1-dependent phosphorylation of Atg9 may recruit Vps34 complex I to the PAS, thereby gathering Atg18, a phosphoinositide-binding protein essential for autophagy, to the PAS. Given this, the above results indicating that Vps34 phosphorylation requires Atg1 kinase (Figure 4) but is dispensable for its own PtdIns3K activity (Figure 3H) prompted us to ask whether Atg1-dependent Vps34 phosphorylation is required for the recruitment of Vps34 complex I to the PAS. To address this question, we analyzed the PAS localization of Atg14 in *vps34* mutants under nitrogen starvation (Figure 6A, B). Contrary to our expectation, the colocalization of Atg14 with Atg13 was not affected in either Vps34[12A] or Vps34[12D] cells, indicating that Vps34 phosphorylation is dispensable for the PAS recruitment of Vps34 complex I. In line with this, the localization of Atg14 to the PAS was also unaffected in *atg1Δ* and *atg1^{D211A}* cells (Figure S6A). We also tested whether Vps34 phosphorylation is involved in the regulation of the PAS formation, since the PAS is strongly accumulated in the absence of *ATG1* [47]. However, we could not observe any evidence of the involvement of Vps34 phosphorylation in the PAS assembly (Figure S6B, C). Collectively, these data indicate that Atg1-dependent phosphorylation of Vps34 is not required for the recruitment of Vps34 complex I to the PAS nor for the PAS assembly.

Because both Atg1 and Vps34 are crucial for targeting Atg18 to the PAS [15,49,53], we then monitored the PAS localization of Atg18 in *atg1* and *vps34* mutants by examining the colocalization of Atg18 with Atg13. As described in a previous report [15], Atg18 could not properly localize to the PAS in the absence of Atg1 or its kinase activity (Figure S6D). Next, we performed the same experiments in *vps34* mutant cells. In wild-type cells, approximately 35% of Atg13 puncta were colocalized with Atg18 (Figure 6C, D). Interestingly, the ratio of Atg13 puncta colocalized with Atg18 was significantly increased in cells expressing the non-phosphorylatable Vps34[12A]. Conversely, cells expressing the phosphomimetic Vps34[12D] showed the PAS targeting of Atg18 comparable to that of wild-type cells. These data suggest that Atg18 is more accumulated at the PAS under nitrogen starvation in the absence of Vps34 phosphorylation. The C-terminal tagging of fluorescent proteins to the Atg proteins used above does not seem to cause a severe defect in autophagy, as shown in Figure S6E.

It has been demonstrated that, without Atg1 kinase activity, Atg8 recycling at the PAS is severely impaired and thus results in prolonged GFP-Atg8 puncta lifetimes [54,55]. The extended GFP-Atg8 puncta lifespan has been also described in cells with defective Atg18 dynamics [56,57]. Given that cells expressing the nonphosphorylatable Vps34[12A] showed Atg18

accumulation at the PAS, we investigated whether GFP-Atg8 puncta lifetime is indeed affected in those cells using time-lapse microscopy. In wild-type cells, GFP-Atg8 puncta lasted for an average of 5.44 min after 6 h of nitrogen starvation (Figure 6E, F). In contrast, GFP-Atg8 puncta in Vps34[12A]-expressing cells lasted for 6.66 min on average, which is approximately 22% longer than the GFP-Atg8 lifespans of wild-type cells. Notably, GFP-Atg8 puncta displaying prominently longer lifetime (≥ 12 min) were observed in Vps34[12A]-expressing cells, while they were absent in cells expressing wild-type Vps34. It is assumable that extension of GFP-Atg8 puncta lifetime causes an increase in the number of Atg8 puncta per cell. In agreement with this assumption, the number of GFP-Atg8 puncta was indeed increased in Vps34[12A]-expressing cells (Figure S6F, G). Collectively, these data suggest that Vps34 phosphorylation is required for normal dynamics of downstream Atg proteins including Atg18 and Atg8 at the PAS.

Discussion

In this study, we show that Vps34 is a substrate of Atg1 kinase and that its phosphorylation is required for the efficient activation of autophagy. Notably, Vps34 with reduced mobility in SDS-PAGE has been reported in both yeast and mammalian systems [21,22]. In addition, the phosphoregulation mechanisms of the Vps34 complex by several kinases, such as CDK and PDK, have been widely explored in mammalian systems [26,58]. Nevertheless, there is only marginal knowledge about the significance of phosphorylation of Vps34 in terms of autophagy regulation. This is probably due to the following natures of this phosphorylation: (i) Vps34 autophosphorylates itself, making it difficult to distinguish passively regulated phosphoresidues from autophosphorylated residues in IP-MS spectra, and (ii) multiple sites are simultaneously phosphorylated, which makes it frustrating to identify specific combinations of residues that are required for autophagy regulation. We tried to circumvent the aforementioned problems by (i) identifying phosphorylation residues through IP-MS using a kinase-dead variant of Vps34 (Figure S2) and (ii) substituting all identified phosphorylation residue candidates with alanine at once (Figure 3A, B). Substitution of three consecutive S/T residues of the 12S/T residues with alanine (Vps34[3A-1] to Vps34[3A-4]) had a minor effect on the mobility shift of Vps34 in SDS-PAGE and autophagy (Figure 3B, D), while Vps34[12A]-expressing cells showed complete loss of mobility shift and defective autophagy. Based on this observation, rather than phosphorylation of particular one or two sites being essential, it is likely that the overall phosphorylation status of the Vps34 helical domain (from S428 to S468) is important for regulating autophagy. Our study is valuable in that it reveals the functional significance of Vps34 phosphorylation in autophagy regulation, which has previously been difficult to uncover.

Our data suggest that Vps34 can be phosphorylated only when stable complex I is formed. Considerable, but not complete, inhibition of Vps34 phosphorylation observed in *atg38Δ* cells (Figure 2A and S1) also supports this notion because a substantial portion of complex I can be assembled in the absence of Atg38 [59]. It has been previously described that Atg38 promotes Vps34 complex I localization to the PAS [21]. Given that the PAS localization of

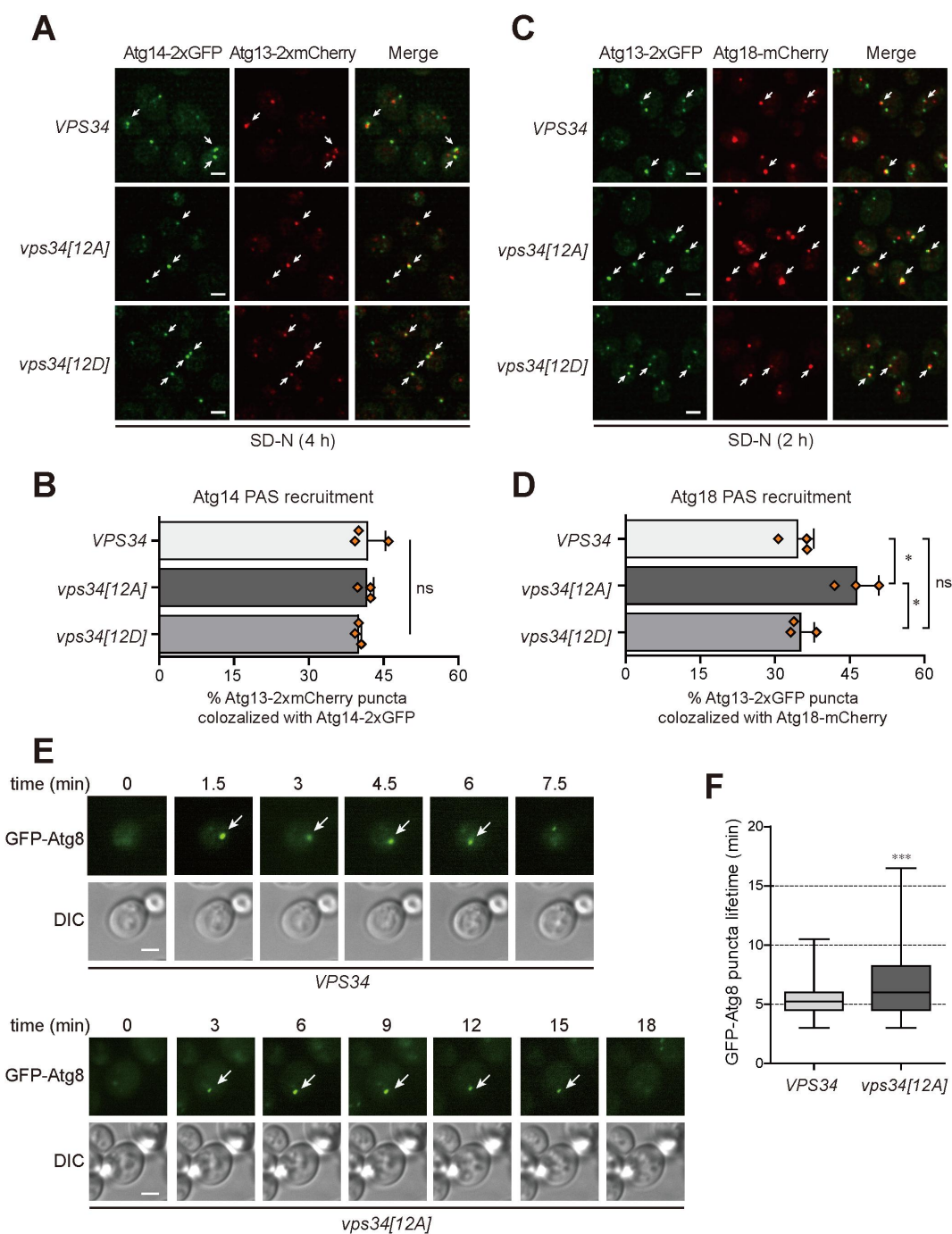


Figure 6. Vps34 phosphorylation is required for normal PAS dynamics. **(A)** Colocalization of Atg14-2xGFP with Atg13-2xmCherry in cells expressing the indicated Vps34 variants was examined after 4 h of incubation in SD-N medium. Colocalized puncta are indicated by white arrows. Scale bars: 2 μ m. **(B)** Quantification of the ratio of Atg13-2xmCherry puncta colocalized with Atg14-2xGFP in **(A)**. At least 150 Atg13-2xmCherry puncta were counted for each measurement. **(C)** Colocalization of Atg18-mCherry with Atg13-2xGFP in cells expressing the indicated Vps34 variants was examined after 2 h of incubation in SD-N medium. Colocalized puncta are indicated by white arrows. Scale bars: 2 μ m. **(D)** Quantification of the ratio of Atg13-2xGFP puncta colocalized with Atg18-mCherry in **(C)**. At least 150 Atg13-2xGFP puncta were counted for each measurement. **(A and C)** Representative z-projected images are shown. **(B and D)** The values represent the averages of three independent experiments. Error bars indicate the standard deviations. Asterisks indicate significant differences compared with WT cells (two-tailed Student's *t*-test): * $p < 0.05$; ** $p < 0.01$; ns, not significant. **(E)** GFP-Atg8-expressing *vps34* Δ cells harboring plasmids expressing WT Vps34 or Vps34[12A] were incubated in SD-N for 6 h and then imaged every 45 s for 40 min. The white arrow indicates the GFP-Atg8 punctum being traced. Scale bars: 2 μ m. **(F)** Box plot depicting the mean lifetimes of GFP-Atg8 puncta shown in **(E)**. Lifetimes of 130 puncta of GFP-Atg8 for each strain were analyzed. The central mark indicates the median, and the bottom and top edges of the box indicate the interquartile range. The box plot whiskers represent the maximum/minimum data points. Asterisks indicate significant differences compared with WT cells (two-tailed Student's *t*-test): *** $p < 0.001$.

Vps34 is necessary for its phosphorylation (Figure 5), it is presumable that one of the major roles of Atg38 in autophagy activation is to promote phosphorylation of Vps34 by (i) holding Vps15-Vps34 and Atg14-Vps30 subcomplexes together, thereby stabilizing the

complex I, and by (ii) guiding Vps34 complex I to the PAS, where Vps34 can be phosphorylated. Consistent with this idea, *atg38* Δ cells show a mild reduction in nonselective autophagic activity but unaffected selective autophagic activity [21], a phenotype similar to

that of the nonphosphorylatable Vps34[12A]-expressing cells in our study. A more detailed relationship between Atg38 and Vps34 phosphorylation remains to be investigated.

In vitro Atg1 kinase assay revealed that the 12S/T residues contain the majority of Atg1 target residues (Figure 4E). However, Atg1 reaction alone could not induce full mobility shift of Vps34 in standard SDS-PAGE (Figure 4C, D), suggesting that Atg1 does not phosphorylate all of the 12S/T residues. Given that Vps34 was not phosphorylated in the absence of Atg1 kinase activity in vivo (Figure 4A, B), it is presumable that, under nitrogen starvation, direct phosphorylation of the Atg1 target sites of Vps34 is a prerequisite for the subsequent phosphorylation of the other part of the 12S/T residues by yet unidentified kinase(s). In this regard, phosphorylation of Vps34 under nitrogen starvation is indeed "Atg1-dependent", and the cooperative action of Atg1 and other unknown kinase(s) seems to be required for the complete phosphorylation of Vps34. Identification of the unknown kinase(s) responsible for Vps34 phosphorylation would be one of the critical issues to be addressed to understand the regulatory mechanism of autophagy.

Our results demonstrate that Atg18 is accumulated at the PAS in Vps34[12A]-expressing cells (Figure 6C, D). This could be due to increased recruitment of Atg18 to the PAS or reduced dissociation of Atg18 from the PAS. In any case, the above results are unexpected in that Atg1 has been reported to recruit Atg18 to the PAS by Atg9 phosphorylation [15]. Given that Atg1-dependent phosphorylation of Atg9 and Vps34 acts in an opposite way in regulating Atg18 localization to the PAS, it seems that fine-tuning of Atg18 dynamics can be achieved in part by spatiotemporal phosphorylation of various Atg1 substrates including Atg9 and Vps34. However, it is still unclear how phosphorylation of Vps34 affects the dynamics of downstream Atg proteins such as Atg18 and Atg8. It has been previously described that PtdIns3P turnover by the PtdIns3P phosphatase Ymr1 is required for the recycling of various Atg proteins [56]. According to that study, Atg18 remains associated with autophagosomes in *ymr1*Δ cells, and the lifetime of Atg8 puncta in *ymr1*Δ cells is longer than that of wild-type cells. Given this, there is a possibility that Vps34 phosphorylation might contribute to the recruitment of Ymr1 to the PAS, thereby inducing PtdIns3P turnover and the recycling of downstream Atg proteins. Alternatively, because part of the Atg18 pool has been described to be located in close proximity with PtdIns3K complex I at the PAS [60], it is also possible that phosphorylated Vps34 complex I might physically repel Atg18, promoting the dissociation of Atg18 from the PAS. A more detailed investigation of how Vps34 phosphorylation is involved in the regulation of the PAS dynamics would be helpful to expand our knowledge about the regulation of the PAS dynamics and autophagy.

10S/T residues of the 12S/T residues (except for S428 and S437) belong to the serine-enriched SUR of the helical domain of Vps34 (from residue 438 to 478) (Figure 3C) [33]. Furthermore, the SUR of Vps34 is predicted to be at the outermost surface of Vps34 complexes (Figure S3A) [33]. Therefore, it is presumable that phosphorylation of this region of Vps34 might regulate the interaction of the complex with other Atg proteins, thereby influencing protein dynamics at the PAS. Notably, the regions in human PIK3C3/VPS34 (from

S422 to E469) [34] and in *Drosophila* Pi3K59F/Vps34 (P422 to A531) [35] corresponding to the SUR in yeast Vps34 are also structurally undefined and enriched in serine residues. Thus, it is assumable that Vps34 homologs in other higher eukaryotes may also be similarly regulated by phosphorylation in this region. Moreover, the corresponding SUR of human PIK3C3/VPS34 contains three serine residues (S448, S452, and S454) homologous to S460, S463, and S465, respectively, in yeast Vps34 [33]. It would be interesting to investigate whether the human PIK3C3/VPS34 complex I also undergoes phosphoregulation similar to that of yeast Vps34.

Materials and methods

Yeast strains, plasmids, and culture conditions

The *S. cerevisiae* strains and plasmids used in this study are listed in Table S1. Strains were constructed by PCR-mediated epitope tagging method or PCR-mediated gene deletion method, or gene integration using yeast integrative vectors. Unless noted, yeast cells were grown in YPD medium (1% yeast extract [Gibco, 212750], 2% peptone [Gibco, 211677], and 2% glucose [Junsei Chemical, 64220-0650]) to mid-log phase for nutrient rich condition. Synthetic complete (SC) medium lacking appropriate amino acids [61] were used as required. For nitrogen starvation, yeast cells grown to mid-log phase in YPD or SC medium were washed with distilled water and incubated in nitrogen starvation medium (SD-N; 0.17% yeast nitrogen base without amino acids and ammonium sulfate [BD Difco, 233520], 2% glucose). For ammonium sulfate replenishment, (NH₄)₂SO₄ (Samchun Chemicals, A0943) was directly added to the culture medium to a final concentration of 0.5% w/v. For amino acid replenishment, a 10× amino acid mixture for SC medium [61] was directly added to the culture to a final concentration of 1 ×. For solid media, 2% agar (BD Difco, 214010) was added. All cultures were incubated at 30°C.

The oligonucleotide primers used in this study are listed in Table S2. To construct the pRG205-VPS34-TAP vector, the PCR product containing *VPS34p-VPS34-TAP* sequence was amplified using the genomic DNA of the *VPS34-TAP* strain as a template and then inserted into the *SacI/KpnI*-digested pRG205 [62] vector by the SLIC method [63]. pRG205 was a gift from Joerg Stelling (Addgene, 64524). *VPS34p* contains the sequence (~1000 bp) upstream of the *VPS34* start codon. To construct the pRS415-ATG1-HA vector, the PCR product containing *ATG1p-ATG1-HA-ACT1t* sequence was amplified using the genomic DNA of the *ATG1-HA* strain as a template and then ligated into the *SpeI/SalI*-digested pRS415 vector by the conventional restriction/ligation method. *ATG1p* contains the sequence (~550 bp) upstream of the *ATG1* start codon. Point mutations to generate Vps34 and Atg1 mutants were introduced by the SLIC method [63] and inverse PCR [64], respectively. To construct the pRS415-VPS30p-VPS30-GFP vector, the PCR product containing *VPS30p-VPS30-GFP-ADH1t* was amplified using the genomic DNA of the *VPS30-GFP* strain as a template and then ligated into the *XbaI/HindIII*-digested pRS415 (ATCC, 87520) vector by the conventional restriction/ligation method. *VPS30p* contains the sequence (~500 bp) upstream of the *VPS30* start codon. Vps30 truncation mutations were introduced by inverse PCR [64]. To construct the

p415ADH-VPS30(WT/ Δ NTD/ Δ BARA)-GFP vectors, the PCR products containing *VPS30(WT/ Δ NTD/ Δ BARA)-GFP* were amplified using the pRS415-VPS30p-VPS30(WT/ Δ NTD/ Δ BARA)-GFP as templates and then ligated into the *XbaI/HindIII*-digested p415ADH (ATCC, 87374) vector. pFA6a-2xGFP-His3MX6 vector was generated in two steps. First, a linker sequence (SGGGGS) was introduced into pFA6a-GFP-His3MX6 by inverse PCR [64] using FA6a-link-GFP-F/FA6a-link-TAG-R primers (Table S2), generating pFA6a-link-GFP-His3MX6. The PCR product containing Link-GFP was amplified using Link-F (*Sall*, noPacI)/GFP+711 R(PacI) primers (Table S2) and then ligated into *Sall/PacI*-digested pFA6a-linker-GFP-His3MX6, generating pFA6a-2xGFP-His3MX6. The corresponding 2xmCherry tagging vector was generated in the same manner.

Western blot analysis

Cell extracts were prepared as previously described [65]. SDS-PAGE and immunoblotting were conducted using standard methods with an HRP-conjugated anti-mouse IgG antibody (Sigma-Aldrich, A9044), an HRP-conjugated anti-rabbit IgG antibody (Sigma-Aldrich, A6154), an HRP-conjugated anti-GFP antibody (Rockland, 600-103-215), an HRP-conjugated anti-MYC antibody (Santa Cruz Biotechnology, SC-40 HRP), an HRP-conjugated anti-HA antibody (Santa Cruz Biotechnology, SC-7392 HRP), and a rabbit anti-Hxk2 antibody (United States Biological, H2035-03). SDS-PAGE with Phos-tag (Wako chemical, AAL-107) was performed following the manufacturer's instructions as previously described [66]. Densitometry determinations of immunoblot images was performed using ImageJ software.

Lambda phosphatase treatment

Cell extracts were treated with lambda phosphatase (New England Biolabs, P0753S) with or without phosphatase inhibitors (1 mM sodium orthovanadate [Sigma-Aldrich, S6508], 10 mM sodium pyrophosphate [Sigma-Aldrich, 221368], 10 mM β -glycerol phosphate [Sigma-Aldrich, G9422], 10 mM sodium fluoride [Sigma-Aldrich, 201154]).

Co-IP assay

Cells were grown in 50 ml of YPD medium to $OD_{600} = 1.0$ and incubated in SD-N medium for the indicated hours. 150 ml culture of YPD medium ($OD_{600} = 1.0$) was used for Co-IP of Atg38-MYC. Cell extracts were prepared as previously described [65]. Cell extracts were incubated with 20 μ l of IgG-Sepharose beads (GE Healthcare, 17-0969-01) overnight at 4°C. Cells without expressing TAP-tagged proteins were used as a negative control. SDS-PAGE and western blot analyses were performed using standard methods with an HRP-conjugated anti-MYC antibody (Santa Cruz Biotechnology, SC-40 HRP) and an HRP-conjugated anti-mouse IgG antibody (Sigma-Aldrich, A9044).

Autophagy analysis

The alkaline phosphatase activity of Pho8 Δ 60 was measured as previously described [36]. The GFP-Atg8 processing assay was performed as previously described [67].

Yeast cell viability assay

Cells were streaked on YPD agar plates, and a single colony was grown in YPD medium overnight. The overnight culture was diluted in YPD medium to $OD_{600} = 0.01$ and grown to $OD_{600} = 1.0$, followed by incubation in SD-N medium. Cell viability was determined by counting colony forming units (CFUs) as previously described [41]. To quantify the survival integral values, the areas under the survival curves were calculated as previously described [42].

In vitro PtdIns3K activity assay

An in vitro PtdIns3K activity assay was performed as previously described with some modifications [25]. Briefly, cells were grown in 200 ml of YPD medium to $OD_{600} = 1.5$ and then incubated in SD-N medium for 6 h. Cell extracts were prepared as described previously [65]. Atg14-containing Vps34 complex I was obtained by immunoprecipitation of Atg14-TAP using 20 μ l of IgG-Sepharose beads (GE Healthcare, 17-0969-01). The acquired immunocomplex was washed three times with lysis buffer [65] and further washed twice with 2.5 \times substrate buffer (75 mM Tris-Cl, pH 7.5, 125 mM NaCl, 12.5 mM $MnCl_2$). Then the beads were incubated with 1 \times substrate buffer containing 250 μ g/ml phosphatidylinositol (Sigma-Aldrich, 79403) at room temperature. The PtdIns3K reactions were started by adding ATP (20 μ M; Sigma-Aldrich, A1852) and incubated for the indicated times with gentle agitation at room temperature. The reactions were then spotted on nitrocellulose membranes (GE healthcare, 10600001). The resulting membrane was blocked with 3% BSA (SERVA Electrophoresis, 11945.04) dissolved in PBS (137 mM NaCl, 2.7 mM KCl, 10 mM Na_2HPO_4 , pH 7.4, 2 mM KH_2PO_4) for 1 h and incubated with 0.5 μ g/ml PI(3)P grip (Echelon Biosciences, G-0302) dissolved in PBS containing 3% BSA and 0.1% Tween 20 (Thermo Fisher Scientific, J20605) overnight at 4°C. After intensive washing, the amount of PI(3)P grip on the membrane was analyzed by immunoblotting using an HRP-conjugated anti-GST antibody (Santa Cruz Biotechnology, SC-138 HRP).

In vitro Atg1 kinase assay

An in vitro Atg1 kinase assay was performed as previously described with some modifications [16]. For the substrates, *atg1 Δ* cells expressing Vps34^{D731N}-MYC (Vps34[KD]-MYC) or Atg13-TAP were grown in 50 ml of YPD medium to $OD_{600} = 1.0$ and then incubated in SD-N medium for 6 h or 1 h, respectively. 200 ml or 70 ml culture of YPD medium ($OD_{600} = 1.0$) were used to purify Atg14-TAP- or Vps38-TAP-immunocomplex, respectively. Cells were lysed as previously described [65]. For preparing Vps34[KD]-MYC, an anti-MYC antibody (Santa Cruz Biotechnology, SC-40) was added to cell extracts and incubated

for 2 h at 4°C. 20 µl of Protein A-Sepharose (GE healthcare, 17–5138-01) was then added and incubated for 2 h at 4°C. TAP-tagged proteins were immunoprecipitated using 20 µl of IgG-Sepharose beads (GE healthcare, 17–0969-01). The beads were washed three times with lysis buffer [65] and two times with 1× kinase buffer (50 mM Tris-Cl, pH 7.5, 75 mM NaCl, 10 mM MgCl₂). The washed beads were used as substrates for the Atg1 kinase assay. To purify Atg1, cells expressing Atg1-HA or Atg1^{D211A}-HA were grown in 2 L of SC medium to OD₆₀₀ ~ 1.5. Cells were lysed as previously described [65], and cell extracts were incubated with 25 µl of an anti-HA antibody (Santa Cruz Biotechnology, SC-7392) for 4 h at 4°C. 160 µl of Protein A-Sepharose beads (GE Healthcare, 17–5138-01) were added to the extracts and incubated overnight at 4°C. The beads were washed three times with lysis buffer and two times with 1× kinase buffer, followed by elution of the bound proteins using HA peptide (Sigma-Aldrich, I2149; 1 mg/ml) dissolved in 1× kinase buffer. The eluted proteins were added to the substrate-bound beads and incubated at 30°C in the presence of 500 µM ATP (Sigma-Aldrich, A1852). Then, the incubated beads were washed twice with ice-cooled 1× kinase buffer, and SDS-PAGE sample buffer was added. The beads were boiled at 75°C for 10 min. Phosphorylation of Atg13-TAP and Vps34-MYC was detected by western blotting using an HRP-conjugated anti-mouse IgG antibody (Sigma-Aldrich, A9044) or an HRP-conjugated anti-MYC antibody (Santa Cruz Biotechnology, SC-40 HRP), respectively.

Fluorescence microscopy analysis

To analyze the PAS recruitment of Atg14 and Atg18 in *vps34* mutants (Figures 6A, C), live cell imaging was performed using a DeltaVision system (Applied Precision) with a 100×/1.512 NA oil immersion objective lens. Cells were placed on the 8-well glass-bottom dish (Thermo Fisher Scientific, 177402) pretreated with concanavalin A (5 µg/ml; Sigma-Aldrich, C7275) for cell immobilization. Images were acquired by collecting a z-stack of 16 pictures with 0.3 µm-distanced focal planes. The acquired images were deconvoluted and projected into one image using the softWorx software (Applied Precision) as previously described [68]. Then representative z-projected images were shown. Live cell imaging except for Figures 6A, C was performed using a Nikon Eclipse E1 microscope with a Plan Fluor 100×/1.30 NA oil immersion objective lens. 96-well glass-bottomed microplates (Matrical Bioscience, MGB096) were pretreated with concanavalin A (5 µg/ml) (Sigma-Aldrich, C7275) for cell adhesion to the plates. For time-lapse microscopy, cells were placed on concanavalin A-treated 96-well glass-bottomed microplates (Matrical Bioscience, MGB096) and imaged every 45s for 40 min at 26°C. Unless noted, images were acquired from a single z-section.

Statistical analysis

The values presented are the means of three independent experiments, and the error bars indicate the standard deviations. Statistical analysis was performed by a two-tailed Student's *t*-test (***p* < 0.001, ***p* < 0.01, **p* < 0.05).

Acknowledgments

We thank members of the Huh laboratory for helpful discussions. We also thank the Proteomics Core Facility at the School of Biological Sciences in Seoul National University, which is supported by the Center for RNA Research, Institute for Basic Science, for LC-MS/MS analysis. This work was supported by the National Research Foundation of Korea (2020R1A5A1018081 and 2021R1A2C1013718).

Disclosure statement

No potential conflict of interest was reported by the author(s).

Funding

This work was supported by the National Research Foundation of Korea [2020R1A5A1018081, 2021R1A2C1013718].

ORCID

Won-Ki Huh  <http://orcid.org/0000-0002-9091-6594>

References

- [1] Reggiori F, Klionsky DJ. Autophagic processes in yeast: mechanism, machinery and regulation. *Genetics*. 2013 Jun;194(2):341–361.
- [2] Feng Y, He D, Yao Z, et al. The machinery of macroautophagy. *Cell Res*. 2014 Jan;24(1):24–41.
- [3] Yang Z, Klionsky DJ. An overview of the molecular mechanism of autophagy. *Curr Top Microbiol Immunol*. 2009;335:1–32.
- [4] Rubinsztein DC, Shpilka T, Elazar Z. Mechanisms of autophagosome biogenesis. *Curr Biol*. 2012 Jan 10;22(1):R29–34.
- [5] Ktistakis NT, Tooze SA. Digesting the expanding mechanisms of autophagy. *Trends Cell Biol*. 2016 Aug;26(8):624–635.
- [6] Mizushima N, Yoshimori T, Ohsumi Y. The role of Atg proteins in autophagosome formation. *Annu Rev Cell Dev Biol*. 2011;27:107–132.
- [7] Noda NN, Fujioka Y. Atg1 FY family kinases in autophagy initiation. *Cell Mol Life Sci*. 2015 Aug;72(16):3083–3096.
- [8] Kabeya Y, Kamada Y, Baba M, et al. Atg17 functions in cooperation with Atg1 and Atg13 in yeast autophagy. *Mol Biol Cell*. 2005 May;16(5):2544–2553.
- [9] Stjepanovic G, Davies CW, Stanley RE, et al. Assembly and dynamics of the autophagy-initiating Atg1 complex. *Proc Natl Acad Sci U S A*. 2014 Sep 2;111(35):12793–12798.
- [10] Fujioka Y, Suzuki SW, Yamamoto H, et al. Structural basis of starvation-induced assembly of the autophagy initiation complex. *Nat Struct Mol Biol*. 2014 Jun;21(6):513–521.
- [11] Kamada Y, Yoshino K, Kondo C, et al. Tor directly controls the Atg1 kinase complex to regulate autophagy. *Mol Cell Biol*. 2010 Feb;30(4):1049–1058.
- [12] Yamamoto H, Fujioka Y, Suzuki SW, et al. The intrinsically disordered protein Atg13 mediates supramolecular assembly of autophagy initiation complexes. *Dev Cell*. 2016 Jul 11;38(1):86–99.
- [13] Hu Z, Raucci S, Jaquenoud M, et al. Multilayered Control of Protein Turnover by TORC1 and Atg1. *Cell Rep*. 2019 Sep 24;28(13):3486–3496 e6.
- [14] Sanchez-Wandelmer J, Kriegenburg F, Rohringer S, et al. Atg4 proteolytic activity can be inhibited by Atg1 phosphorylation. *Nature Commun*. 2017;18:8:Aug.
- [15] Papinski D, Schuschnig M, Reiter W, et al. Early steps in autophagy depend on direct phosphorylation of Atg9 by the Atg1 kinase. *Mol Cell*. 2014 Feb 6;53(3):471–483.
- [16] Kira S, Noguchi M, Araki Y, et al. Vacuolar protein Tag1 and Atg1-Atg13 regulate autophagy termination during persistent starvation in *S cerevisiae*. *J Cell Sci*. 2021 Feb 26;134(4):jcs253682.

- [17] Reidick C, Boutouja F, Platta HW. The class III phosphatidylinositol 3-kinase Vps34 in *Saccharomyces cerevisiae*. *Biol Chem*. 2017 May 1;398(5–6):677–685.
- [18] Ohashi Y, Tremel S, Williams RL. VPS34 complexes from a structural perspective. *J Lipid Res*. 2019 Feb;60(2):229–241.
- [19] Kihara A, Noda T, Ishihara N, et al. Two distinct Vps34 phosphatidylinositol 3-kinase complexes function in autophagy and carboxypeptidase Y sorting in *Saccharomyces cerevisiae*. *J Cell Biol*. 2001 Feb 5;152(3):519–530.
- [20] Obara K, Sekito T, Ohsumi Y. Assortment of phosphatidylinositol 3-kinase complexes–Atg14p directs association of complex I to the pre-autophagosomal structure in *Saccharomyces cerevisiae*. *Mol Biol Cell*. 2006 Apr;17(4):1527–1539.
- [21] Araki Y, Ku WC, Akioka M, et al. Atg38 is required for autophagy-specific phosphatidylinositol 3-kinase complex integrity. *J Cell Biol*. 2013 Oct 28;203(2):299–313.
- [22] Egan DF, Chun MG, Vamos M, et al. Small molecule inhibition of the Autophagy Kinase ULK1 and identification of ULK1 substrates. *Mol Cell*. 2015 Jul 16;59(2):285–297.
- [23] Park JM, Seo M, Jung CH, et al. ULK1 phosphorylates Ser30 of BECN1 in association with ATG14 to stimulate autophagy induction. *Autophagy*. 2018;14(4):584–597.
- [24] Russell RC, Tian Y, Yuan H, et al. ULK1 induces autophagy by phosphorylating Beclin-1 and activating VPS34 lipid kinase. *Nat Cell Biol*. 2013 Jul;15(7):741–750.
- [25] Park JM, Jung CH, Seo M, et al. The ULK1 complex mediates MTORC1 signaling to the autophagy initiation machinery via binding and phosphorylating ATG14. *Autophagy*. 2016;12(3):547–564.
- [26] Furuya T, Kim M, Lipinski M, et al. Negative regulation of Vps34 by Cdk mediated phosphorylation. *Mol Cell*. 2010 May 28;38(4):500–511.
- [27] Yuan HX, Russell RC, Guan KL. Regulation of PIK3C3/VPS34 complexes by MTOR in nutrient stress-induced autophagy. *Autophagy*. 2013 Dec;9(12):1983–1995.
- [28] Kim J, Kim YC, Fang C, et al. Differential regulation of distinct Vps34 complexes by AMPK in nutrient stress and autophagy. *Cell*. 2013 Jan 17;152(1–2):290–303.
- [29] Zhang D, Wang W, Sun X, et al. AMPK regulates autophagy by phosphorylating BECN1 at threonine 388. *Autophagy*. 2016 Sep;12(9):1447–1459.
- [30] Nair U, Thumm M, Klionsky DJ, et al. GFP-Atg8 protease protection as a tool to monitor autophagosome biogenesis. *Autophagy*. 2011 Dec;7(12):1546–1550.
- [31] Stack JH, Emr SD. Vps34p required for yeast vacuolar protein sorting is a multiple specificity kinase that exhibits both protein-Kinase and phosphatidylinositol-specific Pi-3-Kinase activities. *J Biol Chem*. 1994 Dec 16;269(50):31552–31562.
- [32] Lanz MC, Yugandhar K, Gupta S, et al. In-depth and 3-dimensional exploration of the budding yeast phosphoproteome. *Embo Rep*. 2021 Feb 3;22(2):e51121.
- [33] Rostislavleva K, Soler N, Ohashi Y, et al. Structure and flexibility of the endosomal Vps34 complex reveals the basis of its function on membranes. *Science*. 2015 Oct 9;350(6257):aac7365.
- [34] Tremel S, Ohashi Y, Morado DR, et al. Structural basis for VPS34 kinase activation by Rab1 and Rab5 on membranes. *Nat Commun*. 2021 Mar 10;12(1):1564.
- [35] Miller S, Tavshanjian B, Oleksy A, et al. Shaping development of autophagy inhibitors with the structure of the lipid kinase Vps34. *Science*. 2010 Mar 26;327(5973):1638–1642.
- [36] Noda T, Klionsky DJ. The quantitative Pho8Delta60 assay of nonspecific autophagy. *Methods Enzymol*. 2008;451:33–42.
- [37] Motley AM, Nuttall JM, Hettema EH. Pex3-anchored Atg36 tags peroxisomes for degradation in *Saccharomyces cerevisiae*. *EMBO J*. 2012 Jun 29;31(13):2852–2868.
- [38] Kanki T, Kang D, Klionsky DJ. Monitoring mitophagy in yeast: the Om45-GFP processing assay. *Autophagy*. 2009 Nov;5(8):1186–1189.
- [39] Kanki T, Wang K, Cao Y, et al. Atg32 is a mitochondrial protein that confers selectivity during mitophagy. *Dev Cell*. 2009 Jul;17(1):98–109.
- [40] Tsukada M, Ohsumi Y. Isolation and characterization of autophagy-defective mutants of *Saccharomyces cerevisiae*. *FEBS Lett*. 1993 Oct 25;333(1–2):169–174.
- [41] Noda T. Viability assays to monitor yeast autophagy. *Methods Enzymol*. 2008;451:27–32.
- [42] Jung PP, Christian N, Kay DP, et al. Protocols and programs for high-throughput growth and aging phenotyping in yeast. *PLoS One*. 2015;10(3):e0119807.
- [43] Medeiros TC, Thomas RL, Ghillebert R, et al. Autophagy balances mtDNA synthesis and degradation by DNA polymerase POLG during starvation. *J Cell Biol*. 2018 May 7;217(5):1601–1611.
- [44] Pfaffenwimmer T, Reiter W, Brach T, et al. Hrr25 kinase promotes selective autophagy by phosphorylating the cargo receptor Atg19. *Embo Rep*. 2014 Aug;15(8):862–870.
- [45] Abeliovich H, Zhang C, Dunn WA, et al. Chemical genetic analysis of Apg1 reveals a non-kinase role in the induction of autophagy. *Mol Biol Cell*. 2003 Feb;14(2):477–490.
- [46] Matsuura A, Tsukada M, Wada Y, et al. Apg1p, a novel protein kinase required for the autophagic process in *Saccharomyces cerevisiae*. *Gene*. 1997 Jun 19;192(2):245–250.
- [47] Schreiber A, Collins BC, Davis C, et al. Multilayered regulation of autophagy by the Atg1 kinase orchestrates spatial and temporal control of autophagosome formation. *Mol Cell*. 2021 Dec 16;81(24):5066–5081 e10.
- [48] Kinoshita E, Kinoshita-Kikuta E, Takiyama K, et al. Phosphate-binding tag, a new tool to visualize phosphorylated proteins. *Mol Cell Proteomics*. 2006 Apr;5(4):749–757.
- [49] Suzuki K, Kubota Y, Sekito T, et al. Hierarchy of Atg proteins in pre-autophagosomal structure organization. *Genes Cells*. 2007 Feb;12(2):209–218.
- [50] Suzuki SW, Yamamoto H, Oikawa Y, et al. Atg13 HORMA domain recruits Atg9 vesicles during autophagosome formation. *Proc Natl Acad Sci U S A*. 2015 Mar 17;112(11):3350–3355.
- [51] Noda NN, Kobayashi T, Adachi W, et al. Structure of the novel C-terminal domain of vacuolar protein sorting 30/autophagy-related protein 6 and its specific role in autophagy. *J Biol Chem*. 2012 May 11;287(20):16256–16266.
- [52] Papinski D, Kraft C. Atg1 kinase organizes autophagosome formation by phosphorylating Atg9. *Autophagy*. 2014 Jul;10(7):1338–1340.
- [53] Obara K, Sekito T, Niimi K, et al. The Atg18-Atg2 complex is recruited to autophagic membranes via phosphatidylinositol 3-phosphate and exerts an essential function. *J Biol Chem*. 2008 Aug 29;283(35):23972–23980.
- [54] Xie Z, Nair U, Klionsky DJ. Atg8 controls phagophore expansion during autophagosome formation. *Mol Biol Cell*. 2008 Aug;19(8):3290–3298.
- [55] Cheong H, Nair U, Geng JF, et al. The Atg1 kinase complex is involved in the regulation of protein recruitment to initiate sequestering vesicle formation for nonspecific autophagy in *Saccharomyces cerevisiae*. *Mol Biol Cell*. 2008 Feb;19(2):668–681.
- [56] Cebollero E, van der Vaart A, Zhao M, et al. Phosphatidylinositol-3-phosphate clearance plays a key role in autophagosome completion. *Curr Biol*. 2012 Sep 11;22(17):1545–1553.
- [57] Steinfeld N, Lahiri V, Morrison A, et al. Elevating PI3P drives select downstream membrane trafficking pathways. *Mol Biol Cell*. 2021 Jan 15;32(2):143–156.
- [58] Eisenberg-Lerner A, Kimchi A. PKD is a kinase of Vps34 that mediates ROS-induced autophagy downstream of DAPk. *Cell Death Differ*. 2012 May;19(5):788–797.
- [59] Ohashi Y, Soler N, Garcia Ortegon M, et al. Characterization of Atg38 and NRBF2, a fifth subunit of the autophagic Vps34/PIK3C3 complex. *Autophagy*. 2016 Nov;12(11):2129–2144.
- [60] Suzuki K, Akioka M, Kondo-Kakuta C, et al. Fine mapping of autophagy-related proteins during autophagosome formation in *Saccharomyces cerevisiae*. *J Cell Sci*. 2013 Jun 1;126(Pt 11):2534–2544.
- [61] Sherman F. Getting started with yeast. *Methods Enzymol*. 2002;350:3–41.

- [62] Gnugge R, Liphardt T, Rudolf F. A shuttle vector series for precise genetic engineering of *Saccharomyces cerevisiae*. *Yeast*. 2016 Mar;33(3):83–98.
- [63] Jeong JY, Yim HS, Ryu JY, et al. One-step sequence- and ligation-independent cloning as a rapid and versatile cloning method for functional genomics studies. *Appl Environ Microbiol*. 2012 Aug;78(15):5440–5443.
- [64] Silva D, Santos G, Barroca M, et al. Inverse PCR for point mutation introduction. *Methods Mol Biol*. 2017;1620:87–100.
- [65] Shin CS, Huh WK. Bidirectional regulation between TORC1 and autophagy in *Saccharomyces cerevisiae*. *Autophagy*. 2011 Aug;7(8):854–862.
- [66] Chang Y, Huh WK. Ksp1-dependent phosphorylation of eIF4G modulates post-transcriptional regulation of specific mRNAs under glucose deprivation conditions. *Nucleic Acids Res*. 2018 Apr 6;46(6):3047–3060.
- [67] Kim B, Lee Y, Choi H, et al. The trehalose-6-phosphate phosphatase Tps2 regulates ATG8 transcription and autophagy in *Saccharomyces cerevisiae*. *Autophagy*. 2021 Apr;17(4):1013–1027.
- [68] Park I, Kwon MS, Paik S, et al. HDAC2/3 binding and deacetylation of BubR1 initiates spindle assembly checkpoint silencing. *FEBS J*. 2017 Dec;284(23):4035–4050.